

# Probing four orders of magnitude of the diffusion time in porous silica glass with unconventional NMR techniques

German Farrher<sup>a</sup>, Ioan Ardelean<sup>b,\*</sup>, Rainer Kimmich<sup>a</sup>

<sup>a</sup> *Sektion Kernresonanzspektroskopie, Universität Ulm, 89069 Ulm, Germany*

<sup>b</sup> *Technical University from Cluj-Napoca, Physics Department, 400020 Cluj-Napoca, Romania*

Received 17 February 2006; revised 21 June 2006

Available online 21 July 2006

## Abstract

The combined use of two unconventional NMR diffusometry techniques permits measurements of the self-diffusion coefficient of fluids confined in porous media in the time range from 100 microseconds to seconds. The fringe field stimulated echo technique (FFStE) exploits the strong steady gradient in the fringe field of a superconducting magnet. Using a standard 9.4 T (400 MHz) wide-bore magnet, for example, the gradient is 22 T/m at 375 MHz proton resonance and reaches 60 T/m at 200 MHz. Extremely short diffusion times can be probed on this basis. The magnetization grid rotating frame imaging technique (MAGROFI) is based on gradients of the radio frequency (RF) field. The RF gradients not necessarily need be constant since the data are acquired with spatial resolution along the RF gradient direction. MAGROFI is also well suited for unilateral NMR applications where all fields are intrinsically inhomogeneous. The RF gradients reached depend largely on the RF coil diameter and geometry. Using a conic shape, a value of at least 0.3 T/m can be reached which is suitable for long-time diffusion measurements. Both techniques do not require any special hardware and can be implemented on standard high RF power NMR spectrometers. As an application, the influence of the tortuosity increasing with the diffusion time is examined in a saturated porous silica glass.

© 2006 Elsevier Inc. All rights reserved.

**Keywords:** NMR; Diffusion; Porous media; Radiofrequency gradients; Fringe field gradients; Pulse field gradients

## 1. Introduction

The most popular principle of NMR diffusion measurements is based on the attenuation of spin echoes due to incomplete refocusing of coherences as a consequence of incoherent molecular displacements during the pulse sequence. Echo attenuation on these grounds arises in the presence of pulsed or steady gradients of the main magnetic flux density. Any sort of gradient-based echo can be used. Typical examples are the Hahn and the stimulated echo [1–3]. Here we consider the stimulated echo arising after three RF pulses in the presence of the steady fringe field gradient of a superconducting magnet. The method will be called fringe field stimulated echo (FFStE) technique.

On the other hand, there are methods employing gradients of the amplitude of the radio frequency flux density, i.e. RF field gradients [4]. Such an alternative protocol for diffusion measurements was successfully demonstrated with rotating-frame echo phenomena [3–7]. Furthermore,  $B_1$  and  $B_0$  gradients can be applied in mixed form. If suitably matched, such mixed combinations of gradients lead to “nutation echoes” [8,9] the diffusive attenuation of which can also be used for molecular displacement studies [10]. The localized character of nutation echoes [9] in principle permits remote measurements of diffusion coefficients. Moreover, it may be possible to accomplish diffusion measurements with chemical shift resolution in inhomogeneous static magnetic fields [11], provided that the directions of  $B_1$  and  $B_0$  gradients coincide.

With the techniques mentioned so far, a non-equilibrium magnetization distribution is first prepared in the form of a “helix” or—with respect to a certain component—as a

\* Corresponding author. Fax: +40 264 401 536.

E-mail address: [ioan.ardelean@phys.utcluj.ro](mailto:ioan.ardelean@phys.utcluj.ro) (I. Ardelean).

magnetization “grid” (or “grating”). Translational diffusion then tends to level the magnetization distribution during the diffusion time. This leveling process of the magnetization grid can be monitored globally via the attenuation of spin echoes. Diffusion coefficients can then be evaluated from echo attenuation curves.

An alternative protocol is to render the magnetization profile along the gradient direction in the form of a one-dimensional image. Such a technique was proposed in Refs. [12,13] and termed magnetization grid rotating-frame imaging (MAGROFI). The appealing advantage of the MAGROFI technique in comparison with other rotating frame techniques based on rotary or nutation spin echoes is that no spatially constant gradient is required. As the magnetization grid is rendered as an image, it is only the local gradient that is relevant for the evaluation of diffusion constants. That is, the coil geometry can be optimized for strong gradients regardless of homogeneity requirements. Favorable coil geometries to be used for diffusion measurements with the MAGROFI technique turned out to be solenoids [13], conic coils [8,14] or a toroid cavity detector [15,16].

The present study focuses on the ability of the FFStE and MAGROFI techniques to probe the time dependence of the diffusion coefficient in a porous glass saturated with liquid water. The total time range to be covered with this sort of sample system is four orders of magnitude from 100  $\mu$ s to 1 s. The time dependence of the self-diffusion coefficient of fluids in saturated and unsaturated porous glasses is of particular interest since it provides information on the topological constraints, the tortuosity of the pore space and the exchange dynamics between the phases.

## 2. Methodological background

### 2.1. The fringe-field stimulated echo technique

The principle of FFStE diffusometry is well-documented in the literature [1–3] and will not be discussed in detail here. We only mention that the RF pulse sequence used in the experiments reads

$$\frac{\pi}{2} - \tau_1 - \frac{\pi}{2} - \tau_2 - \frac{\pi}{2} - \tau_1 - \text{acquisition},$$

where  $\tau_1 > T_2^*$  and  $T_2^*$  is the time constant of the FID attenuation in the presence of  $B_0$  inhomogeneities. For the suppression of base-line offsets and undesired signals, the following phase cycles was used:

First RF pulse	$x$	$x$	$-x$	$-x$	$x$	$x$	$-x$	$-x$
Second RF pulse	$y$	$-y$	$x$	$-x$	$x$	$-x$	$y$	$-y$
Third RF pulse	$y$	$-y$	$x$	$-x$	$x$	$-x$	$y$	$-y$

The RF pulse width was 1.8  $\mu$ s so that 1 mm thick slices of the sample were excited in a fringe field gradient of 22 T/m.

For  $\tau_2$  intervals comparable with  $\tau_1$ , the diffusion time is defined by  $t_{\text{diff}} \equiv \frac{2}{3}\tau_1 + \tau_2 = \text{const}$  (compare Table 19.1 in

Ref. [1], where the attenuation factors for diverse field gradient diffusometry techniques are given). The influence of transverse and longitudinal relaxation can be accounted for either by employing one of the diverse self-compensating pulse sequences reported in the literature [17–19] or by measuring the relaxation times separately and dividing the stimulated-echo amplitude by the corresponding factors. Since a well-defined diffusion time is of interest in the present study, we have preferred the latter measuring protocol.

### 2.2. The MAGROFI technique

The MAGROFI technique is based on RF field gradients [12,13]. In the following the principles of this technique will be outlined in order to clarify how the technique can be best adapted for time dependent diffusion measurements. The basic pulse sequence of a MAGROFI experiment is indicated in Fig. 1. Three intervals can be distinguished: preparation of the magnetization grid, diffusion interval and imaging of the grid. A single RF coil produces all RF pulses needed. That is, the spatial distribution of their RF fields and consequently the field gradients are identical. The RF flux density is assumed along the  $x'$  axis in the frame rotating with the resonance frequency  $\omega_r = \omega_0 = \gamma B_0$ . In the treatment, all interactions among the spins will be neglected. It is also assumed that gradients of the main magnetic field ( $B_0$  gradients) of external or internal (i.e. susceptibility induced) origin neither affect the excitation of the spins nor give rise to further diffusive signal attenuation in the imaging interval. This implies that all local offsets of the main magnetic field,  $\Delta B_0(\vec{r}) \equiv B(\vec{r}) - B_0$ , should be negligible relative to the amplitude of the RF field,  $B_1(\vec{r})$ .

The shortest diffusion interval is limited by the free induction decay time  $T_2^*$ . If  $\tau_2 < 5 T_2^*$ , some hard-to-control deviations from the proper coherence pathway would occur. Diffusive displacements during the preparation and imaging intervals (see Fig. 1) can be neglected if the RF pulses are much shorter than the diffusion interval. Otherwise, a formalism analogous to the well-known Stejskal/Tanner treatment for finite field gradient pulses [1–3] may be employed. In this case, the diffusion time is again defined by  $t_{\text{diff}} \equiv \frac{1}{3}\tau_1 + \tau_2 = \text{const}$ . In the following, we will however assume the short-pulse limit  $\tau_1 \ll \tau_2$  for simplicity,

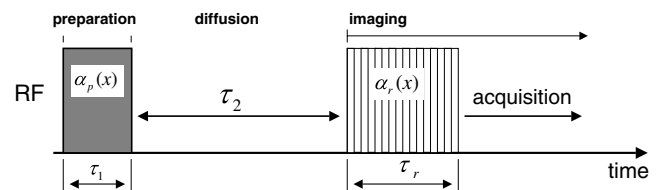


Fig. 1. The basic pulse sequence of the MAGROFI technique. The first RF gradient pulse produces a magnetization grid that will be leveled by diffusive displacements during the diffusion interval. Rotating-frame imaging of the magnetization grid permits the evaluation of self-diffusion coefficients and relaxation times.

so that diffusion effects during RF gradient pulses need not be considered, and the diffusion time can be approximated as  $t_{\text{diff}} \approx \tau_2$ .

The effect of the first RF pulse on the equilibrium magnetization  $M_0$  is a precession around the  $x'$  axis of the rotating frame. The local nutation angular frequency is  $\omega_1(x) = \gamma B_1(x)$  assuming that the gradient of the RF amplitude is directed along the  $x$  axis of the laboratory frame. The magnetization components after the preparation pulse can be obtained for instance as solutions of Bloch equations [1]. The transverse components (i.e. spin coherences) are spoiled in the diffusion interval by  $B_0$  gradients due to imperfect shimming and transverse relaxation. The only component that survives the interval  $\tau_2$  is the  $z'$  magnetization, where longitudinal relaxation times long enough for the generation of finite signals ( $T_1 \gg \tau_1$ ) are anticipated. In the limit of short and intense RF gradient pulses, so that the conditions

$$\tau_1 \ll T_2 \quad \text{and} \quad \omega_1 T_2 \gg 1 \quad (1)$$

are fulfilled ( $T_2$  is the transverse relaxation time), the local  $z'$  magnetization at  $t = \tau_1$ , immediately after the preparation pulse of variable duration  $\tau_1$  is given by [12,13]:

$$M_{z'}(x, \tau_1) \approx M_0 \cos[\gamma B_1(x) \tau_1]. \quad (2)$$

In the interval  $\tau_2$ , diffusive displacements of the molecules tend to level the  $z'$  magnetization grid created by the first RF pulse. Independently of diffusion, longitudinal relaxation further modifies the magnetization grid with the tendency to reach homogeneously the equilibrium magnetization. Assuming a Gaussian distribution of displacements [1] characterized by a diffusion coefficient,  $D$ , the  $z'$  magnetization at the end of the diffusion interval is given by [12,13],

$$M_{z'}(x, \tau_1 + \tau_2) = M_0 \cos[\gamma B_1(x) \tau_1] e^{-D[\gamma G_1(x)]^2 \tau_1^2 \tau_2} e^{-\frac{\tau_2}{T_1}} + M_0 \left(1 - e^{-\frac{\tau_2}{T_1}}\right), \quad (3)$$

where  $T_1$  is the longitudinal relaxation time and  $G_1(x) = |\partial B_1(x)/\partial x|$  is the local magnitude of the  $B_1$  gradient. The first term in the above expression represents the partially leveled magnetization grid while the second term refers to the fraction of magnetization recovered by longitudinal relaxation.

In the derivation of the above expression it has been assumed that the local gradient is constant over regions larger than the root mean squared displacement in the diffusion interval. Note that, the magnetization is to be measured with spatial resolution so that diffusivities are determined locally. In principle, the diffusion coefficient may be different for different  $x$  positions but the propagator that describes the molecular migration must always be Gaussian.

The second RF pulse (reading pulse) of variable duration  $\tau_r$  transfers the longitudinal magnetization, Eq. (3), into a longitudinal and a transverse component. Again, the effects can be accounted for by solving the Bloch equa-

tions [1]. The only component of the magnetization that produces signals in the receiver coil is the transverse component. In the limits described by Eq. (1), the transverse component after the application of the reading pulse is given by

$$M_{y'}(x, \tau_1 + \tau_2 + \tau_r) = \left\{ M_0 \cos[\gamma B_1(x) \tau_1] e^{-D[\gamma G_1(x)]^2 \tau_1^2 \tau_2} e^{-\frac{\tau_2}{T_1}} + M_0 \left(1 - e^{-\frac{\tau_2}{T_1}}\right) \right\} \sin[\gamma B_1(x) \tau_r]. \quad (4)$$

The signal, i.e., the amplitude of the free-induction decay following the RF pulse is a superposition of signals of all volume elements along the  $B_1$  gradient direction (here  $x$  direction). This represents an average of the transverse component over the sample dimensions and is proportional to

$$S(\tau_r) = \int_{\text{sample}} f(x) \left\{ M_0 \cos[\gamma B_1(x) \tau_1] e^{-D[\gamma G_1(x)]^2 \tau_1^2 \tau_2} e^{-\frac{\tau_2}{T_1}} + M_0 \left(1 - e^{-\frac{\tau_2}{T_1}}\right) \right\} \sin[\gamma B_1(x) \tau_r] dx. \quad (5)$$

The factor  $f(x)$  accounts for the distribution of the detection sensitivity of the coil.

According to Eq. (5) the magnetization grid shape function can be reproduced by Fourier transformation to the  $x$  domain. Note however that if the RF gradients are not constant but position dependent, a simple numerical FFT procedure cannot be applied for extracting the magnetization grid. In this case the magnetization grid can be obtained from the integral  $\int S(\tau_r) e^{i\gamma B_1(x) \tau_r} d\tau_r$  over the whole time domain (acquisition interval). This situation applies also to our RF coil.

The rotating frame images of the magnetization grid permit the evaluation of the local diffusion coefficients provided that the local gradients,  $G_1(x)$ , are known. If the RF gradients are inhomogeneous, i.e. if  $B_1(x)$  is not a linear function of  $x$ , the spatial distribution of the RF field has to be accounted for in the Fourier transform. The  $B_1(x)$  distribution can either be calculated from the coil geometry or measured by conventional  $B_0$  gradient imaging techniques monitoring the excitation distribution induced by the RF coil.

In order to obtain a one-dimensional image of the magnetization grid for a given diffusion time, transients with incremented reading pulse lengths  $\tau_r$  must be recorded as Eq. (5) suggests. This may be a time consuming procedure. It is therefore more favorable to employ the fast, single-shot variant described in Refs. [13,16]. The method consists of a series of short gradient pulses with narrow intervals in between permitting the stroboscopic acquisition of data points of the pseudo FID (see Fig. 2). Each RF pulse can be understood as an increment of the previous RF pulses taken together. Thus the whole information needed for the Fourier transform evaluation of the magnetization grid can be recorded in one transient of the pulse train. In principle, RF gradient techniques are well suited for chemical shift resolved diffusion studies. However, this

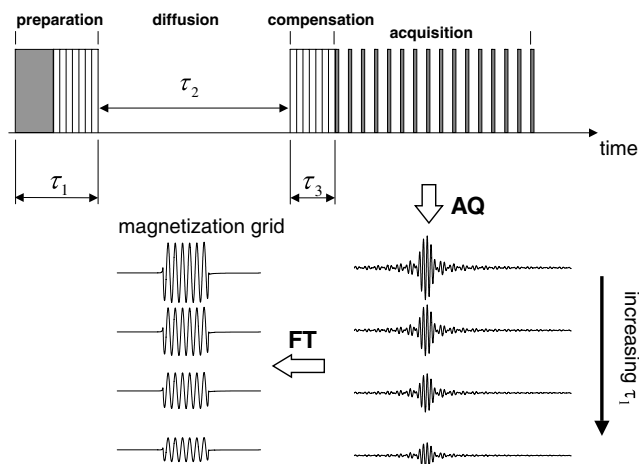


Fig. 2. Practical RF gradient pulse scheme of the MAGROFI experiment used in the present study. The preparation pulse is incremented in subsequent transients from a starting value of 180  $\mu\text{s}$  in 32 steps of  $\tau_r = 20 \mu\text{s}$  each. The magnetization grid produced by the preparation pulse is read after the diffusing interval by a rapid rotating frame imaging technique. The compensation pulse stretches the magnetization grid effectively imaged so that the wavelength of the modulation is always constant independent of the preparation pulse length.

option must be sacrificed when employing pulse trains such as the one described above.

In a typical MAGROFI diffusion experiment, the signal is recorded as a function of the width (or amplitude) of the preparation pulse. That is, the width (or the amplitude) of the preparation RF pulse is incremented in subsequent experiments [12]. After the interval  $\tau_2$ , the grid is rendered as an image, and the magnitude of the magnetization is measured at the desired position. From such data, the diffusion coefficient is evaluated according to

$$A(x, \tau_1) = A_0 \cos[\gamma B_1(x) \tau_1] e^{-D[\gamma G_1(x)]^2 \tau_1^2} e^{-\frac{\tau_2}{\tau_1}}. \quad (6)$$

This, however, may be a tedious procedure since the grid modulation wavelength varies with the preparation pulse length (see Eq. (4)).

It is therefore more practical to employ a compensation RF pulse prior to the reading pulse. The compensation pulse is varied in the same way as the preparation pulse. The grid image rendered in this way thus has always the same wavelength (see Fig. 2), and the evaluation of diffusion coefficients can be focused on the region of interest. The compensation pulse makes up for the variable part of the preparation pulse before the grid is imaged using the rapid rotating frame imaging method [13,16]. Note that in this case the diffusion time must be defined as  $t_{\text{diff}} \equiv \frac{1}{3} \tau_1 + \tau_2 + \frac{1}{3} \tau_3 = \text{const}$  due to the presence of a third diffusion period  $\tau_3$ .

### 3. The experimental implementation and results

All experiments were carried out at room temperature and at 9.4 T using a conventional Bruker spectrometer with a 89 mm bore. The sample, a porous silica glass termed VitraPor#5 was purchased from ROBU Glasfilter-Geräte

GmbH, Germany. The nominal mean pore size is  $d = 1 \mu\text{m}$  ( $\pm 0.6 \mu\text{m}$ ), the specific surface area is  $1.75 \text{ m}^2/\text{g}$ , and the porosity is specified as  $\Phi = 0.43$ . The samples were pretreated as suggested by the manufacturer (see Ref. [20]) and then saturated with distilled water.

For the fringe field stimulated echo measurements an ordinary high-power probe with a solenoid RF coil was placed about 15.5 cm below the middle of the magnet. At this position, a steady field gradient of 22 T/m at 375 MHz proton resonance frequency was reached. The gradient was calibrated by measuring the diffusion coefficient of bulk water at room temperature. The thickness of the selected slice of the sample was 1 mm. The fringe field flux density was measured with the aid of a home made Hall probe.

In order to measure the echo attenuation due to diffusion, the interval  $\tau_1$  was varied between 10 and 80  $\mu\text{s}$  in 32 steps. Since  $T_2^* \approx 1.2 \mu\text{s}$  in the presence of the strong fringe field gradient, extremely short diffusion times could be examined. Under the conditions of our samples, this turned out to be about 100  $\mu\text{s}$ . Even shorter diffusion times would be reachable if the maximum fringe field gradient of our magnet, 60 T/m, would have been employed. However, under such experimental conditions, the detection sensitivity is much worse and does not permit sensitive studies of porous glasses especially if partially filled.

In order to produce favorable  $B_1$  gradients for the MAGROFI technique, the RF coil of an ordinary probehead of the system was replaced by a conic coil (see Fig. 3a). The same coil was used for detection and rotating frame imaging. The dimensions and number of turns of the coil together with the position and dimensions of the cylindrical sample are given in Fig. 3a. The  $B_1(x)$  field distribution on the coil axis was measured by imaging a disc shaped sample of 0.5 mm thickness. With the aid of a mechanical device, this test sample was manually moved along the coil axis. The  $B_1$  value at each position on the coil axis was determined from the image of the sample using the MAGROFI pulse sequence without preparation pulse. From the spatial distribution of the  $B_1$  values, local RF gradients  $G_1(x)$  were evaluated. The data for  $B_1(x)$  (circles) and  $G_1(x)$  (continuous line) are shown in Fig. 3b. Calculations based on Biot/Savart's law confirmed that the homogeneity of the  $B_1(x)$  and  $G_1(x)$  values in planes perpendicular to the coil axis are homogeneously distributed within the lateral area occupied by the samples.

The RF gradient preparation pulse was varied between 180 and 820  $\mu\text{s}$  in 32 steps. The compensation pulses were synchronously increased between 0 and 640  $\mu\text{s}$ . One-dimensional rapid rotating frame images were rendered by acquiring a pseudo free-induction decay with a train of 200 pulses, each of 2  $\mu\text{s}$  duration followed by stroboscopic acquisition of the signals between the pulses. The Fourier transform of the pseudo free-induction decay produces the magnetization distribution as schematically shown in Fig. 2. The  $B_1(x)$  field distribution given in Fig. 3b was used for the numerical Fourier transformation procedure.

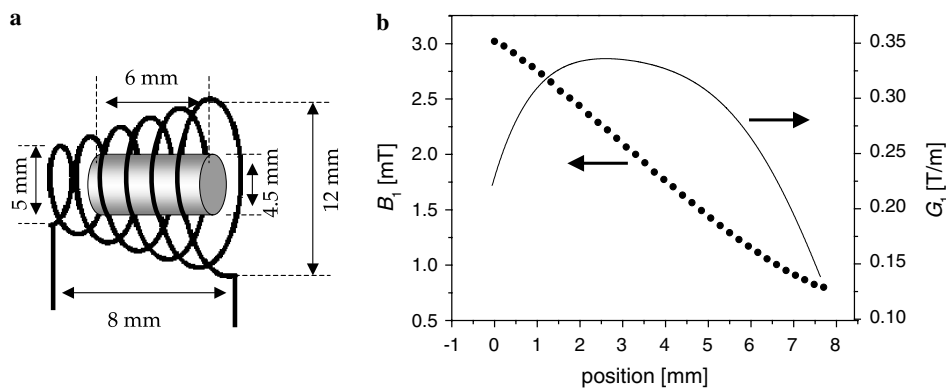


Fig. 3. (a) The conic coil used for the generation of the RF gradient field. (b) The measured amplitude of the RF magnetic flux density  $B_1$  (circles) at different positions along the coil axis and the calculated local  $B_1$  gradient (continuous line). The  $B_1$  data have been measured by NMR imaging with the aid of a 0.5 mm thick water sample mechanically shifted in 36 steps along the coil axis. The  $G_1$  values were derived numerically from the  $B_1$  data.

The decay curves were found to be monoexponential in the frame of the experimental accuracy as expected for constant gradients in the evaluated region of interest. The diffusion coefficient was finally evaluated on the basis of Eq. (6). The shortest diffusion time is determined by  $T_2^*$ , as discussed above.

Fig. 4 shows experimental data recorded with the FFStE and MAGROFI diffusometry techniques on water saturating Vitrapor#5 porous sample and bulk water. The data coincide in the overlap regions of the applicability of the two methods. This demonstrates that results acquired with these methods are equally reliable. Moreover, the correctness of the experimental protocol and of the definition of the diffusion time at short pulse intervals is corroborated in this way.

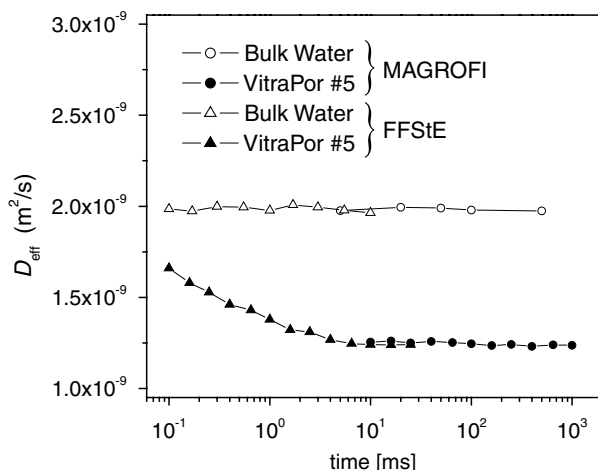


Fig. 4. Diffusion coefficient of water in saturated VitraPor#5 and in bulk at room temperature versus the effective diffusion time  $t_{\text{diff}}$ . In the case of saturated VitraPor#5 sample geometrical restrictions more and more obstruct diffusion with increasing diffusion time. The triangles indicate the data measured with the FFStE technique. The circles refer to the MAGROFI technique. The diffusion times for the FFStE and MAGROFI techniques defined by  $t_{\text{diff}} = \frac{2}{3}\tau_1 + \tau_2$  and  $t_{\text{diff}} = \frac{1}{3}\tau_1 + \tau_2 + \frac{1}{3}\tau_3$ , respectively, account for echo attenuation by diffusion during the encoding intervals. They were kept constant in each experiment.

The accessible diffusion time windows are shifted relative to each other. The shortest diffusion times can be probed with the fringe field stimulated echo method. It is demonstrated that under the conditions of samples like water, diffusion times less than 100  $\mu\text{s}$  can safely be reached. On the other hand, due to the finite switching and eddy current settling times, the conventional pulsed field gradient stimulated echo technique turned out to fail with diffusion times below 10 ms.

The short-time limit of the MAGROFI diffusometry method is determined by the condition  $\tau_2 \gg T_2^*$  and the assumption of negligible diffusion and relaxation effects during the RF gradient pulses. The long-time limit is commonly determined by spin-lattice relaxation, that is in the case of our sample  $t_{\text{diff}} \approx 1$  s.

#### 4. Discussion and conclusions

Two different field gradient NMR diffusometry techniques have been compared in the context of a study of the time dependence water diffusion in saturated porous glasses. The quality of the diffusion data is comparable in both cases. However, the ranges of the accessible diffusion times strongly deviate from each other. That is, if a particularly wide experimental diffusion time window is required, one has to combine the two techniques. In the present study, we have demonstrated that the combination of FFStE and MAGROFI diffusometry methods permits one to cover four orders of magnitude of the diffusion time.

The techniques are limited at short diffusion times by the magnitude of the available field gradient and by the FID decay time  $T_2^*$ . In this respect, the FFStE is optimal and definitely superior to the MAGROFI method. Under the present conditions, the shortest diffusion time for which MAGROFI provided reliable results was 5 ms compared to 100  $\mu\text{s}$  in the FFStE case.

Another question is how demanding and costly the experimental set-up is to reach the desired specifications of the system. Both with the FFStE and MAGROFI techniques, no special hardware such as pulsed gradient units

and gradient coils are needed. Solid state NMR spectrometers can be used in the standard configuration apart from potentially some minor modifications of probeheads.

The MAGROFI technique is based on RF field gradients. Unlike the rotary echo method discussed in Refs. [4–6], the gradients need not be constant. Since a rotating-frame imaging technique is used, diffusion coefficients can be evaluated at a desired position along the gradient direction based on the local  $B_1$  gradient value. This facilitates the design of RF gradient coils for specific applications. In principle, even standard RF coils with solenoidal geometry, for instance, can be used without any modification by placing the sample in the fringe field of the coil where the  $B_1$  gradient is strong enough.

The switching times of RF pulses are intrinsically short. Eddy currents in metal components of the probehead are not excited perceptibly. No magnetic susceptibility force impulse is exerted on the sample by RF gradient pulses. The preparation interval is kept as short as principally possible. The latter means that instead of exciting coherences by a  $90^\circ$  pulse, applying a  $B_0$  gradient pulse, and “storing” the encoded transverse magnetization along the  $z'$  direction with the aid of the second  $90^\circ$  pulse of the FFStE sequence, a single RF gradient pulse is applied in the preparation interval of the MAGROFI technique.

A further point to be mentioned here is that  $B_1$  gradient techniques are not susceptible to artifacts by  $B_0$  field inhomogeneities caused by magnetic susceptibility distributions or simply imperfect shimming. The only condition is that the RF amplitude is larger than the field offsets in the sample [21]. This point is of particular importance for more recent developments of so-called unilateral NMR applications where  $B_0$  fields are intrinsically inhomogeneous [22].

## Acknowledgments

This work was supported by the Alexander von Humboldt Foundation, the Deutsche Forschungsgemeinschaft and the Romanian MEC.

## References

- [1] R. Kimmich, NMR Tomography, Diffusometry, Relaxometry, Springer-Verlag, Berlin, 1997.
- [2] J. Kärger, H. Pfeifer, W. Heink, Principles and applications of self diffusion measurements by nuclear magnetic resonance, *Adv. Magn. Reson.* 12 (1988) 1–89.
- [3] I. Ardelean, R. Kimmich, Principles and unconventional aspects of NMR diffusometry, *Annu. Rep. NMR Spectrosc.* 49 (2003) 43–115.
- [4] D. Canet, Radiofrequency field gradient experiments, *Prog. NMR Spectrosc.* 30 (1997) 101–135.
- [5] F. Humbert, M. Valtier, A. Retournard, D. Canet, Diffusion measurements using radiofrequency field gradient: artifacts, remedies, practical hints, *J. Magn. Reson.* 134 (1998) 245–254.
- [6] R. Dupeyre, Ph. Devoulon, D. Bourgeois, M. Decorps, Diffusion measurements using stimulated rotary echoes, *J. Magn. Reson.* 95 (1991) 589–596.
- [7] P. Maffei, P. Mutzenhardt, A. Retournard, B. Diter, R. Raulet, J. Brondeau, D. Canet, NMR microscopy by radio-frequency field gradients, *J. Magn. Reson. A* 107 (1994) 40–49.
- [8] I. Ardelean, A. Scharfenecker, R. Kimmich, Two pulse nutation echoes generated by gradients of the radiofrequency amplitude and of the main magnetic field, *J. Magn. Reson.* 144 (2000) 45–52.
- [9] I. Ardelean, R. Kimmich, A. Klemm, The nutation spin echo and its use for localised NMR, *J. Magn. Reson.* 146 (2000) 43–48.
- [10] A. Scharfenecker, I. Ardelean, R. Kimmich, Diffusion measurements with the aid of nutation spin echoes appearing after two inhomogeneous radiofrequency pulses in inhomogeneous magnetic fields, *J. Magn. Reson.* 148 (2001) 363–366.
- [11] D. Topgaard, A. Pines, Self-diffusion measurements with chemical shift resolution in inhomogeneous magnetic fields, *J. Magn. Reson.* 168 (2004) 31–35.
- [12] R. Kimmich, B. Simon, H. Köstler, Magnetization-grid rotating frame imaging technique for diffusion and flow measurements, *J. Magn. Reson.* 112 (1995) 7–12.
- [13] B. Simon, R. Kimmich, H. Köstler, Rotating frame imaging technique for spatially resolved diffusion and flow studies in the fringe field of RF probe coils, *J. Magn. Reson. A* 118 (1996) 78–83.
- [14] J.P. Boehmer, R.I. Prince, R.W. Briggs, The cone coil, an RF gradient coil for spatial encoding along the  $B_0$  axis in rotating-frame imaging experiments, *J. Magn. Reson.* 83 (1989) 152–159.
- [15] K. Woelk, B.L.J. Zwank, P. Trautner, E. Lehnhof, J. Bargon, R.J. Klingler, R.E. Gerald II, J.W. Rathke, Finite-difference approach for the high precision analysis of rotating-frame diffusion images, *J. Magn. Reson.* 145 (2000) 276–290.
- [16] P. Trautner, K. Woelk, Improved strategies for NMR diffusion measurements with magnetization grating rotating frame imaging (MAGROFI), *Phys. Chem. Chem. Phys.* 4 (2002) 5973–5981.
- [17] R. Kimmich, E. Fischer, One- and two-dimensional pulse sequences for diffusion experiments in the fringe field of superconducting magnets, *J. Magn. Reson. A* 106 (1994) 229–235.
- [18] D.E. Demco, A. Johansson, J. Tegenfeldt, Constant-relaxation methods for diffusion measurements in the fringe field of superconducting magnets, *J. Magn. Reson. A* 110 (1994) 183–193.
- [19] E. Fischer, R. Kimmich, Constant time steady gradient NMR diffusometry using the secondary stimulated echo, *J. Magn. Reson.* 166 (2004) 273–279.
- [20] I. Ardelean, G. Farrher, C. Mattea, R. Kimmich, Nuclear magnetic resonance study of the vapour contribution to silica glasses with micrometer pores partially filled with liquid cyclohexane and water, *J. Chem. Phys.* 120 (2004) 9809–9816.
- [21] R. Raulet, J.M. Escanye, F. Humbert, D. Canet, Quasi-immunity of  $B_1$  gradient NMR microscopy to magnetic susceptibility distortions, *J. Magn. Reson. A* 119 (1996) 111–114.
- [22] F. Casanova, J. Perlo, B. Blümich, K. Kremer, Multi-echo imaging in highly inhomogeneous magnetic fields, *J. Magn. Reson.* 166 (2004) 76–81.